# THz ANTENNA-COUPLED ZERO-BIAS SCHOTTKY DIODE DETECTORS FOR PARTICLE ACCELERATORS

R. Yadav[1,*], S. Preu, Terahertz Devices and Systems, TU Darmstadt, Darmstadt, Germany
A. Penirschke, High Frequency Tech., Mittelhessen Univ. of Applied Sciences, Friedberg, Germany
J. Michael Klopf, M. Kuntzsch, Helmholtz-Zentrum Dresden-Rossendorf, Dresden, Germany
[1]also at High Frequency Tech., Mittelhessen Univ. of Applied Sciences, Friedberg, Germany

## Abstract

Semiconductor-based broadband room-temperature Terahertz (THz) detectors are well suitable for beam diagnosis and alignment at accelerator facilities due to easy handling, compact size, no requirement of cooling, direct detection and robustness. Zero-Bias Schottky Diode (ZBSD) based THz detectors are highly sensitive and extremely fast, enabling the detection of picosecond scale THz pulses. This contribution gives an overview of direct THz detector technologies and applications. The ZBSD detector developed by our group has undergone several tests with table-top THz sources and also characterized with the free-electron laser (FEL) at HZDR Dresden, Germany up to 5.56 THz. In order to understand the rectification mechanism at higher THz frequencies, detector modelling and optimization is essential for a given application. We show parametric analysis of a antenna-coupled ZBSD detector by using 3D electromagnetic field simulation software (CST). The results will be used for optimization and fabrication of next generation ZBSD detectors, which are planned to be commissioned at THz generating FEL accelerator facilities in near future.

## INTRODUCTION

The electromagnetic spectrum from 0.1 to 10 THz was commonly known as terahertz (THz) gap until recently as rigorous research and development have led to develop sources, detectors and components which help to bridge the THz gap [1]. Among available tabletop THz sources, accelerator based sources such as free electron lasers (FEL), synchrotrons and linear particle accelerators generate coherent as well as non-coherent THz signals [2]. THz signals can be used for various applications such as spectroscopy, study of matters, medical imaging, etc. [3]. THz detectors plays a crucial role in order to harness the full power of THz signals in various applications. These detectors can be classified into several categories based on their working principles (such as thermal detectors, electrical detectors etc. [1]), operating ranges (frequency of coverage for example narrow or broadband [1]) and operating conditions (room temperature or cryogenic conditions [1, 4–8]). There has been a rigorous work for the development of Schottky diode for THz applications [7, 9–11].

Zero-Bias Schottky Diode (ZBSD) based THz detectors are an end product of combination of ZBSD, antenna, planar electronic components and post detection electronics.

* rahul.yadav@iem.thm.de

Therefore, the overall performance of the ZBSD detector is dependent on all these components. In order to optimize the ZBSD THz detectors, in this paper we focus on the investigation of planar antennas for antenna-coupled ZBSD detector, which is planned to be primarily commissioned at ELBE facility in Helmholtz Zentrum Dresden-Rossendorf (HZDR), Germany and other facilities too.

## SIGNAL RECTIFICATION IN ZBSD

For conventional Schottky diodes, the external bias $V$ modifies the Schottky barrier height, which led the electrons to cross the barrier and ultimately led to set the operating point of Schottky diode by reducing differential resistance ($R_{diff}$) [11, 12]. In case of ZBSD, the material is engineered in such a way that at $V = 0$ sufficient electrons are able to cross the barrier, yet with sufficient non-linearity of the IV characteristics to cause rectification. The ZBSD used for the detector development in our group are fabricated on Indium Gallium Arsenide (InGaAs) substrate which have electron affinity of 4.5 eV. Due to the proprietary reason by ACST GmbH, the in-depth information of Schottky diode itself is out of context of this paper. The ZBSD used here feature a quasi-vertical structure for Schottky and ohmic contact [9], rather than either having only planar or only vertical structure [11].

The signal rectification takes place at the Schottky contact of ZBSD, which can be understand by using Taylor series [13] as follows: The incident (monochromatic) Terahertz wave is transformed to a bias by the antenna as

$$U_0(t) = U_0 \cos(\omega t) \tag{1}$$

where $U_0(t)$ is the signal with amplitude $U_0$ and angular THz frequency $\omega$. By using the Taylor series expansion of the exponential diode characteristic up-to second order, the diode current $I_0$ becomes

$$I_0(t) = A_1 U_0 \cos(\omega t) + A_2 U_0^2 \cos^2(\omega t) + .... \tag{2}$$

$$= A_1 U_0 \cos(\omega t) + \frac{1}{2} A_2 U_0^2 + \frac{1}{2} A_2 U_0 cos(2\omega t) \tag{3}$$

where the second term in Eq. (3) is the DC term. The first and second terms are derived from diode characteristics [11]:

$$A_1 = \frac{1}{R_{diff}} \tag{4}$$

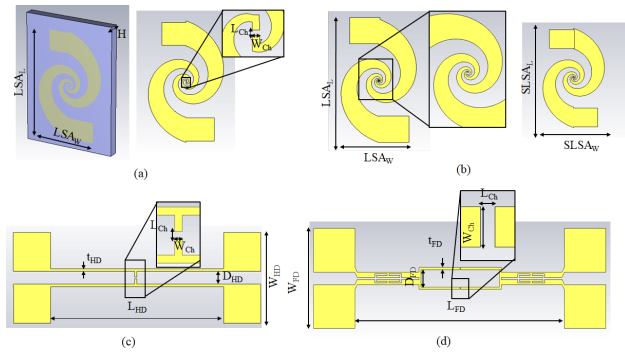$$A_2 = \frac{1}{2 \cdot R_{diff} \cdot \eta \cdot U_T} \tag{5}$$

Figure 1: Sketch of the antennas investigated for ZBSD THz detectors (inset shows the central part where ZBSD is coupled) (a) left: antenna with substrate view, right: 1.5 turns log spiral antenna, (b) left: 2.5 turns log-spiral antenna, right: 1.5 turns smaller-log spiral antenna, (c) H-dipole antenna and (d) Folded dipole antenna. Note: antennas are excited using discrete port in CST between two electrodes in channel $L_{Ch} \times W_{Ch}$, where practically ZBSD is located.

where in Eq. (5), $\eta$ is diode ideality factor and $U_T$ is semiconductor (InGaAs) thermal voltage. As the second order term contains a rectified component $I_D C = A_2 U_0^2$, $A_2$ is directly proportional to the responsivity of the ZBSD.

## ANTENNA-COUPLED ZBSD DETECTOR

The antenna plays a crucial role in the performance of the detector because it couples the incident THz radiation to the ZBSD, where it gets rectified. Planar antennas are used in this work to couple the ZBSD for detector development. The selection of the antenna depends on the desired application and required bandwidth. Table 1 shows different types of antennas which are used for the development of ZBSD THz detector.

Table 1: Investigated Antenna for ZBSD THz Detector

| S.No | Antenna type | Abbreviation |
|------|--------------|--------------|
| 1 | Log-spiral | LSA |
| 2 | Small log-spiral | SLSA |
| 3 | H-dipole | HD |
| 4 | Folded dipole | FD |

The LSA and SLSA are self-complimentary, frequency-independent antennas, which means theoretically they have no limitation on operational bandwidth. However, practically the upper bandwidth limitation is defined by the innermost arm radius and lower frequency by outermost arm radius [14] as shown in Fig. 1 (a) and (b).

We also investigated antenna types that are frequently applied in Terahertz photomixers, such as the H-dipole (HD) antenna (Fig. 1 (c)). In this type of antenna, either the central bar (high frequencies) the arm structure (low frequencies) radiates as the wave propagates along it. These type of antennas are considered as broadband antennas. In order to increase the detector sensitivity in narrow-band operation, investigations on performance of folded dipole (FD) anten-

Table 2: Dimensions of the Structures

| Abbre-viation | Full form | Dimension [µm] |
|---------------|-----------|----------------|
| $LSA_L$ | Log-spiral antenna length | 1174.25 |
| $LSA_W$ | Log-spiral antenna width | 557.60 |
| H | Substrate height | 4.5 |
| $L_{Ch}$ | Channel length | 2.4, 3, 6, 8 |
| $W_{Ch}$ | Channel width | 2.4, 10 |
| $SLSA_L$ | Small log-spiral antenna length | 413.14 |
| $SLSA_W$ | Small log-spiral antenna width | 200.90 |
| $L_{HD}$ | H-dipole antenna length | 700 |
| $W_{HD}$ | H-dipole antenna width | 350 |
| $D_{HD}$ | H-dipole antenna arm distance | 50 |
| $t_{HD}$ | H-dipole antenna arm thickness | 10 |
| $W_{FD}$ | Folded-dipole antenna width | 458 |
| $L_{FD}$ | Folded-dipole antenna length | 1020 |
| $D_{FD}$ | Folded-dipole antenna arm distance | 80 |
| $t_{FD}$ | Folded-dipole antenna arm thickness | 10 |

nas were also performed (Fig. 1 (d)).The dimensions of the investigated antennas are mentioned in Table 2.

The ZBSD will be fabricated on an Indium Gallium Arsenide (InGaAs) substrate which is equivalent to the area mentioned by $L_{Ch} \times W_{Ch}$ in the Fig. 1. The ZBSD will be integrated with the antenna, which will be fabricated on the film-thin substrate of 4.5 µm thickness and dielectric constant of $|\varepsilon_r| = 2.8$.

## RESULTS AND DISCUSSION

The dielectric constant of the material on which antenna-coupled ZBSD is fabricated plays an important role in the performance of the detector. According to babinet's principle [14], the radiation impedance ($Z_A$) of self-complimentary antenna (LSA and SLSA) is inversely proportional to its effective refractive index ($n_{eff}$) and thus to its dielectric constant as

$$Z_A = \frac{Z_0}{2 \cdot n_{eff}} \quad (6)$$

$$Z_A = \frac{Z_0}{\sqrt{2 \cdot (\varepsilon_1 + \varepsilon_2)}} \quad (7)$$

where, $Z_0$ is the wave impedance in free space (377 Ω), $\varepsilon_1$ is dielectric constant of free space (1) and $\varepsilon_2$ is dielectric constant of thin-film substrate (2.8). Considering the respective values of ZBSD fabrication material, unloaded radiation resistance is $Z_A$=137 Ω. Figure 2, shows the effect of $|\varepsilon_r|$ variation on the performance of LSA antenna with $10 \times 8$ µm$^2$ channel when exciting the antenna from the center (where ZBSD is located), which directly relates to the ZBSD detector performance as well. The $|S_{11}|$ (scattering parameters in the channel $L_{Ch} \times W_{Ch}$ where practically ZBSD is located) shows standing waves for almost all $|\varepsilon_r|$ until 0.6 THz due to the inductive part of the antenna being dominant (Fig. 2(d)), while above 0.6 THz the imaginary part of radiation impedance becomes capacitive which leads
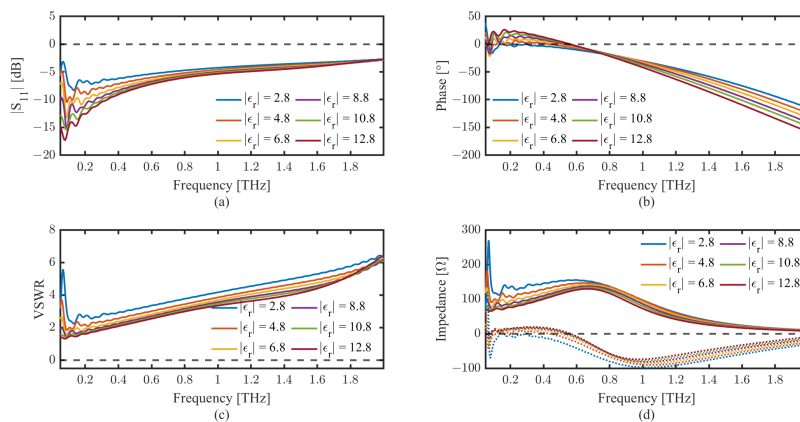
Figure 2: Effect of variable $|\varepsilon_r|$ on LSA antenna with $10 \times 8\ \mu m^2$ channel with ZBSD having $C_j = 1$ fF and $R_{diff} = 5$ kΩ, (a) $|S_{11}|$, (b) Phase response, (c) VSWR response and (d) Impedance, solid lines represent real part and dotted lines represent imaginary part.
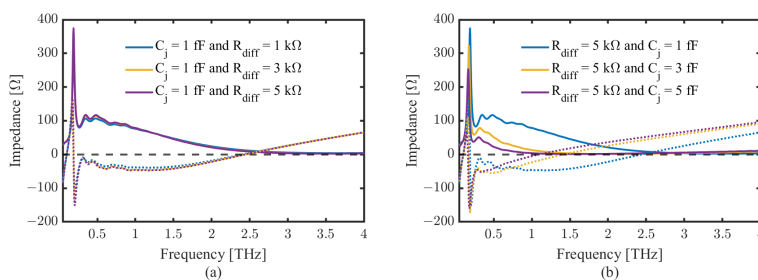


Figure 3: (a) Total device impedance for constant $C_j = 1$ fF and variable $R_{diff}$, (b) Total device impedance for variable $C_j$ and constant $R_{diff} = 5$ kΩ with SLSA antenna with $2.4 \times 2.4\ \mu m^2$ channel. Dotted lines: imaginary part, solid lines: real part of impedance, on substrate of 4.5 μm thickness and dielectric constant of $|\varepsilon_r| = 2.8$.

to sign flip of phase (Fig. 2(b)). The voltage standing wave ratio (VSWR) is almost below 3 up to 0.8 THz and then increases gradually to 6 at 2 THz (Fig. 2(b)), which means as frequency increases the capacitive part of the radiation impedance become significantly important.

The junction capacitance ($C_j$) and differential resistance ($R_{diff}$) are the important parameters of ZBSD which effect the antenna performance as a function of frequency. Fig. 3(a) shows the variation of $R_{diff}$ while keeping the $C_j = 1$ fF constant. The variation in differential resistance does not affect the radiation impedance of the detector. As the frequency increases, the capacitive part of impedance become inductive after 2.5 THz. This is because the wavelength is reaching towards the same dimension of the central electrodes (where the ZBSD is coupled). When in the case of $R_{diff}$ is kept constant at 5 kΩ and $C_j$ is variable (Fig. 3(b)), the radiation impedance of the antenna is changed significantly. The lower the junction capacitance $C_j$ is, the higher is the real part of radiation impedance and longer the frequency range over which the imaginary part stays capacitive before becoming inductive. This proves that it is important to have lower $C_j$ to have better responsivity of the device at higher THz frequency. Therefore, we selected to consider $C_j = 1$ fF and $R_{diff} = 5$ kΩ for remaining studies in this work.

Figure 4 shows the radiation impedance versus frequency response from 0.05 to 4 THz (except LSA $2.4 \times 2.4\ \mu m^2$ which is from 0.05 to 2 THz only) with variable channel dimensions of $10 \times 3\ \mu m^2$, $10 \times 6\ \mu m^2$ and $2.4 \times 2.4\ \mu m^2$ for all the four types of antennas considered for investigation in this study. LSA with channel dimension of $10 \times 3\ \mu m^2$ and $10 \times 6\ \mu m^2$ have real $Z_A$ of 133 Ω at lower frequencies (0.05 THz), which further decreases to 50 Ω at 1 THz (Fig. 4 (a)). The smaller channel dimension of $2.4 \times 2.4\ \mu m^2$ have real $Z_A$ of 268 Ω at 0.069 THz and decreases to approximately 100 Ω at 1 THz. This shows the better device response with smaller channel dimensions for LSA type devices. The smaller log-spiral devices (SLSA) are 2.84 times smaller in length compared to LSA devices. The SLSA devices in Fig. 4 (b) shows the resonance behaviour around 0.1 THz for all the three channel dimensions, which afterwards drop of real ($Z_A$) to 78 Ω for $2.4 \times 2.4\ \mu m^2$ channel and almost 50 Ω for both $10 \times 3\ \mu m^2$ and $10 \times 6\ \mu m^2$ channel. While the real part is almost similar for $10 \times 3\ \mu m^2$ and $10 \times 6\ \mu m^2$ (as observed in Fig. 4 (a) and (b)), the imag ($Z_A$) shows the smaller channel length have slightly prolonged capacitive behaviour. The H-dipole antenna has resonances at 0.16, 0.38 and 0.61 THz as shown in Fig. 4 (c) for all studied channel dimensions. The HD with $2.4 \times 2.4\ \mu m^2$ have real ($Z_A$) of 2.3 kΩ compared to approx 1.9 kΩ for both $10 \times 3\ \mu m^2$ and $10 \times 6\ \mu m^2$ channel at 0.16 THz. The folded dipole antenna (FD) is a narrow band resonant having the resonance peak at 0.2 THz as shown in Fig. 4 (d). This type of antenna can be used to boost up the device responsivity at particular frequency for a very specific frequency selective application.
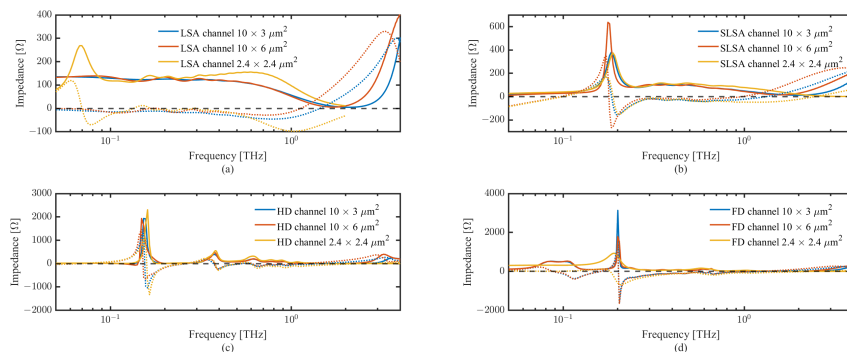
Figure 4: Antenna radiation impedance versus frequency response for variable channel dimensions of (a) 1.5 turn log-spiral antenna, (b) 1.5 turn small log-spiral antenna, (c) H-dipole antenna and (d) folded-dipole antenna from 0.05 to 4 THz. Dotted lines: imaginary part, solid lines: real part of radiation impedance, on substrate of 4.5 μm thickness and dielectric constant of $|\varepsilon_r|$ = 2.8.
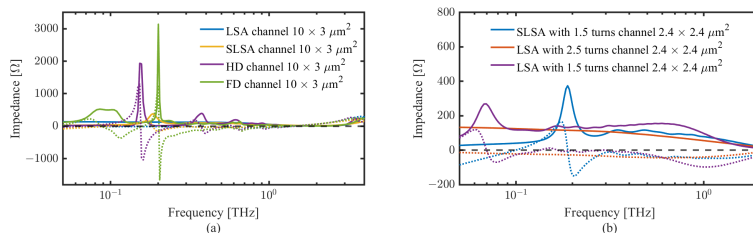


Figure 5: (a) Comparison of radiation impedance of all the four investigated antennas with channel dimension of $10 \times 3$ μm$^2$ from 0.05 to 4 THz and (b) comparison of log-spiral antennas with channel dimension of $2.4 \times 2.4$ μm$^2$ from 0.05 to 2 THz. Dotted lines: imaginary part, solid lines: real part of radiation impedance, on substrate of 4.5 μm thickness and dielectric constant of $|\varepsilon_r|$ = 2.8.

Figure 5 (a) compares the impedance response for all four types of antennas with channel dimension of $10 \times 3$ μm$^2$ (this channel dimension is used for comparison because a device with smaller channel length has comparatively better response). Clearly the HD and FD devices are the best option for frequency selective improvement due to their resonant behaviour at specific frequencies. The LSA and SLSA devices are the best choice for broadband applications, however with frequency their responsivity decreases [7]. As shown in Fig. 6, the device reponsivity decreases as $f^{-6}$ towards higher THz frequencies. On comparing the LSA and SLSA antennas impedance for $2.4 \times 2.4$ μm$^2$ channel dimension, it is observed that both antennas have resonant peaks at 0.07 and 0.2 THz, respectively. The response for LSA is higher than SLSA at lower frequencies as expected, but above approx. 1 THz, the response of SLSA is slightly better as shown in Fig. 5 (b). The antenna with 2.5 turns features non-resonant behaviour and response decreases gradually over frequency. It does not have any prominent inductive component.
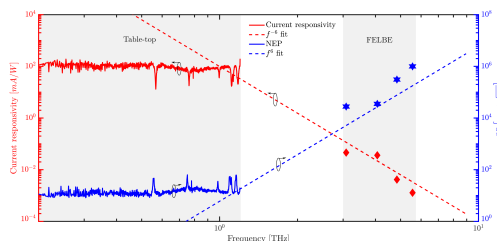


Figure 6: Responsivity of the log-spiral antenna-coupled broadband THz detector [7].

channel dimension in antenna design in this paper. The proper selection of $C_j$ and $R_{diff}$ is important for the better device response. The selection of the antenna type is often a trade-off between its responsivity and operational bandwidth. Short channel dimensions (here $10 \times 3$ μm$^2$ and $2.4 \times 2.4$ μm$^2$) are best choices for future device fabrication. The antenna studies presented here provide the expected performance of the optimized ZBSD detectors to be fabricated in the near future under this project.

## CONCLUSION

In this paper, we investigated the importance of antenna selection and design based on the desired operational bandwidth. At higher THz frequency, typical antenna sizes are much bigger compared to the THz wavelength incident on the detector, therefore only the central electrodes play a crucial role. We investigated and showed the importance of

## ACKNOWLEDGEMENT

# REFERENCES

[1] G. Carpintero, E. Garcia-Munoz, H. Hartnagel, S. Preu, and A. Raisanen, *Semiconductor terahertz technology: devices and systems at room temperature operation*, John Wiley & Sons, 2015. `doi:10.1002/9781118920411`

[2] E.J. Jaeschke, S. Khan, J.R. Schneider, and J.B. Hastings, *Synchrotron light sources and free-electron lasers: Accelerator physics, instrumentation and science applications*, 2nd Edition, Cham: Springer International Publishing, 2020. `doi:10.1007/978-3-030-23201-6`

[3] H.J. Song and T. Nagatsuma, *Handbook of terahertz technologies: devices and applications*, CRC press, 2015. `doi:10.1201/b18381.`

[4] S. Preu, M. Mittendorff, S. Winnerl, O. Cojocari, and A. Penirschke, "THz Autocorrelators for ps Pulse Characterization Based on Schottky Diodes and Rectifying Field-Effect Transistors", *IEEE Trans. Terahertz Sci. Technol.*, vol. 5, no. 6, pp. 922-929, Nov. 2015. `doi:10.1109/TTHZ.2015.2482943`

[5] S. Regensburger, S. Winnerl, J.M. Klopf, H. Lu, A.C. Gossard, and S. Preu, "Picosecond-Scale Terahertz Pulse Characterization With Field-Effect Transistors", *IEEE Trans. Terahertz Sci. Technol.*, vol. 9, no. 3, pp. 262-271, May 2019. `doi:10.1109/TTHZ.2019.2903630`

[6] A. Penirschke *et al.*, "Compact quasi-optical Schottky detector with fast voltage response", in *Proc. 39th IRMMW-THz*, 2014, pp. 1-2. `doi:10.1109/IRMMW-THz.2014.6956027`

[7] R. Yadav *et al.*, "State-of-the-Art Room Temperature Operable Zero-Bias Schottky Diode-Based Terahertz Detector Up to 5.56 THz", *Sensors*, vol. 23, no. 7, p. 3469. `doi:10.3390/s23073469`

[8] J.L. Hesler and T.W. Crowe, "Responsivity and noise measurements of zero-bias Schottky diode detectors", in *Proc. ISSTT*, 2007, pp. 89-92. `https://api.semanticscholar.org/CorpusID:9361326`

[9] O. Cojocari, C. Sydlo, H.-L. Hartnagel, S. Biber, J. Schur, and L.-P. Schmidt, "Schottky–structures for THz-application based on quasi-vertical design-concept", in *Proc. 16th Int. Symp. Space THz Technol.*, pp. 490–495, May 2005. `https://api.semanticscholar.org/CorpusID:108540009`

[10] I. Mehdi, J.V. Siles, C. Lee, and E. Schlecht, "THz Diode Technology: Status, Prospects, and Applications", in *Proc. IEEE'17*, vol. 105, no. 6, pp. 990-1007, Jun. 2017. `doi:10.1109/JPROC.2017.2650235`

[11] M. Hoefle, "Concepts and Design of Zero-bias Schottky Detectors for Millimetre Wave Applications", PhD thesis, TU Darmstadt, Germany, Shaker Verlag, 2015. `doi:10.2370/9783844039405`

[12] A.Y.C. Yu, "The metal-semiconductor contact: an old device with a new future", *IEEE Spectr.*, vol. 7, no. 3, pp. 83–89, Mar. 1970. `doi:10.1109/MSPEC.1970.5213256`

[13] D.M. Pozar, *Microwave Engineering*, John Wiley & Sons, 2011. `ISBN:978-0-470-63155-3`

[14] C.A. Balanis, *Antenna theory: analysis and design*, John Wiley & Sons, 2016. `doi:10.1002/9780470294154`